Fermi Surface and Electronic Structure of $Nd_{2-x}Ce_xCuO_{4-\delta}$

D. M. King,[1] Z.-X. Shen,[1,2] D. S. Dessau,[1,2] B. O. Wells,[1,2] W. E. Spicer,[1] A. J. Arko,[3] D. S. Marshall,[1] J. DiCarlo,[2] A. G. Loeser,[2] C. H. Park,[2] E. R. Ratner,[2] J. L. Peng,[4] Z. Y. Li,[4] and R. L. Greene[4]

[1]*Stanford Electronics Laboratory and Stanford Synchrotron Radiation Laboratory, Stanford University, Stanford, California 94305*

[2]*Department of Applied Physics, Stanford University, Stanford, California 94305*

[3]*Los Alamos National Laboratory, Los Alamos, New Mexico 87545*

[4]*Center for Superconducting Research, Department of Physics, University of Maryland, College Park, Maryland 20742*

(Received 18 December 1992)

Using angle-resolved photoemission, we have mapped out the Fermi surface (FS) of single crystal $Nd_{2-x}Ce_xCuO_{4-\delta}$ when doped as a superconductor ($x=0.15$) and overdoped as a metal ($x=0.22$). The measured FS agrees very well with local-density-approximation calculations and appears to shift with electron doping as expected by a band-filling scenario. The observed FS shape suggests that a model Hamiltonian with only nearest-neighbor interactions is not sufficient to describe the electronic structure near E_F; next-nearest-neighbor interactions should also be considered.

PACS numbers: 79.60.Bm, 73.20.Dx, 74.72.Jt

In the family of high-T_c cuprate superconductors, $Nd_{2-x}Ce_xCuO_{4-\delta}$ (NCCO) has many unique characteristics which make it will suited for study. First of all, it is the only known n-type high-T_c superconductor. In addition, with only one CuO_2 plane per unit cell, no chain states, and no apical oxygen atoms, it is the least complicated of the cuprates. Many of its physical properties exhibit rather conventional behavior, in contrast to the abnormal properties seen in the p-type cuprates of $YBa_2Cu_3O_{7-\delta}$ (YBCO) and $Bi_2Sr_2CaCu_2O_{8+\delta}$ (Bi2:2:1:2). For example, in NCCO the resistivity has a T^2 temperature dependence, indicative of Fermi-liquid behavior [1–3], the tunneling data appear to yield meaningful $\alpha^2F(\omega)$ information [4], and the temperature dependence of the penetration depth and the surface resistivity has been fitted by a simple s-wave BCS function [5]. This is in sharp contrast to the much more complicated picture emerging from YBCO and Bi2:2:1:2 [6–9]. Finally, its optimal T_c is about 25 K, comparable with some conventional low-T_c superconductors. This unique behavior of NCCO reveals the urgent need for a detailed study of its Fermi surface (FS) and electronic structure to elucidate the origin of the physical properties of this relatively simple single-layer compound when compared to the more complicated cuprates such as YBCO and Bi2:2:1:2.

Over the past two years, angle-resolved photoemission (ARPES) has played a key role in revealing the FS and electronic structure of the p-type cuprates. It is generally accepted now that, despite compelling evidence for correlation effects, the FS of the p-type superconductors agrees well with the local-density-approximation (LDA) calculations [10–14]. The calculated FS of the p-type cuprates has also been verified by other experimental techniques such as the deHaas-van Alphen (dHvA) and positron annihilation experiments [15,16]. For NCCO, on the other hand, no experiments have succeeded in revealing FS information. The positron annihilation experiment is difficult in this case because the positrons do not reside near the metallic CuO_2 planes, resulting in a very weak signal from the FS, and the dHvA experiment on NCCO is nontrivial because the scattering rate is still high at low temperatures. ARPES experiments have been performed on NCCO in the past [17]; however, they have not yet succeeded in revealing any FS information.

By using high quality single-crystal samples cleaved in UHV at low temperatures, we have succeeded in mapping the FS of NCCO in the normal state. We see bands crossing E_F at approximately the same locations in the Brillouin zone as predicted by LDA calculations. The measured FS is very simple, in striking contrast to the much more complicated Fermi surfaces of YBCO and Bi2:2:1:2 [12,13,18]. With increased electron doping, we see the FS shift in qualitative agreement with a simple band-filling scenario. In addition, the large density of states observed near E_F at G_1 in YBCO and Bi2:2:1:2 [13,18], thought to arise from a van Hove singularity at the FS, is not observed in NCCO. These findings are particularly important since this is the first time the FS of a one-layer compound has been studied, allowing us to unambiguously investigate the electronic structure of the essential CuO_2 plane.

The single crystals of NCCO were grown from a CuO-based flux. A mixture of starting materials consisting of Nd_2O_3, CeO_2, and CuO was heated rapidly to a maximum temperature just above the melting point (1250–1350 °C depending on the Ce concentration). After a soak of several hours at the maximum temperature, the materials were cooled slowly to room temperature. Free standing crystals were formed with sizes ranging from $2\times2\times0.01$ mm^3 to $10\times10\times0.1$ mm^3. To induce superconductivity, the crystals were placed next to a fresh titanium sponge and annealed at 850 °C in flowing

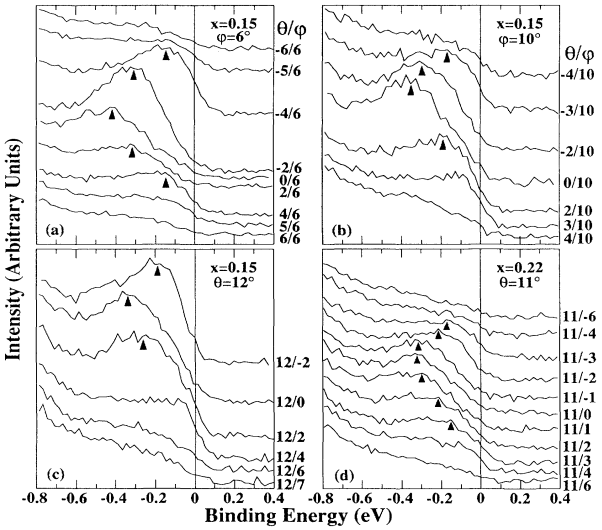

FIG. 1. ARPES data from NCCO for $x=0.15$ (superconductor) and $x=0.22$ (overdoped metal).

argon for 14 h. The best superconducting crystals were obtained near $x=0.15$ with a sharp transition ($\Delta T_c=0.5$ K) at $T_c=25$ K as determined by magnetization and resistivity measurements. The metallic samples, with $x=0.22$, were also characterized by transport and structural analysis tools. More details concerning the sample preparation are contained elsewhere [19].

ARPES experiments on NCCO were carried out at the newly commissioned undulator beam line 5 of the Stanford Radiation Laboratory (SSRL). The experiments were performed using a Vacuum Science Workshop ARPES chamber with $\pm 1°$ angular resolution. The energy resolution for the data presented here is 140 meV, limited by the relatively high photon energy (70 eV) used. The chamber base pressure during the experiments was $\sim 1\times 10^{-10}$ Torr. We cleaved and measured the samples at several temperatures, 25, 35, and 80 K, and the FS information was identical at these different temperatures. We noticed that the samples cleaved at 80 K had fewer steps on the surfaces, but the -9 eV peak, known to be extrinsic to the sample, was found to develop much faster at this temperature. The development of this "dirt" peak was not found to affect the peak position near the Fermi energy. All the data presented in this paper were collected using 70 eV photons. We also verified key Fermi crossing points using 40 eV photons.

Figure 1 presents ARPES data near E_F from NCCO when doped as a superconductor, $x=0.15$, and overdoped as a metal, $x=0.22$. The emission angles θ and ϕ determine $\mathbf{k}_\parallel$ of the collected photoelectrons. Since $\mathbf{k}_\parallel$ is conserved at the solid-vacuum interface, by choosing the appropriate emission angles we specify the desired location in the Brillouin zone that we would like to probe in this quasi-2D material. The grid in Fig. 2 displays the relationship between θ,ϕ and locations in the Brillouin zone. As seen in Fig. 1, the constant-ϕ and constant-θ scans are always taken with both positive and negative angles, and the spectra properly exhibit the crystal symmetry about the Γ-G_1-Z line. For example, in the $\theta=11°$ scan of the metallic sample ($x=0.22$), Fig. 1(d), the peak positions in the spectra with positive φ angles are nearly identical to the positions at the corresponding negative φ angles. The band reaches the maximum binding energy at $\varphi=0°$, disperses towards lower binding energy as we move in $\mathbf{k}$ space towards X, and finally passes through E_F at $\varphi=\pm 4°$. The locations where the dispersive band crosses E_F determine the experimental FS. We use the criteria for a crossing point that the peak has dispersed so that the Fermi energy is located from one-half to two-thirds up the lower binding energy side of the feature and the peak intensity has suddenly diminished. This observed symmetry with respect to the Γ-G_1-Z line is an excellent

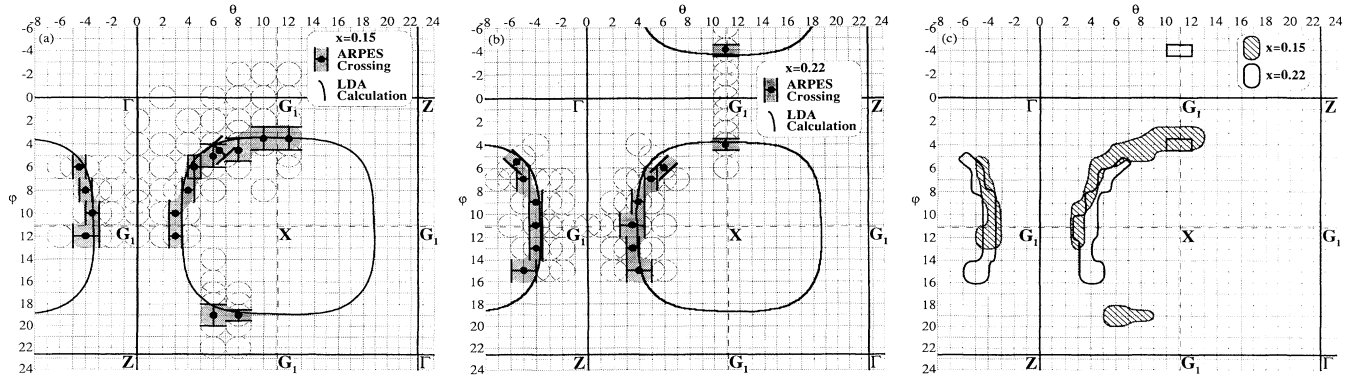

FIG. 2. Experimental FS compared with results from LDA calculations [20] for (a) $x=0.15$ and (b) $x=0.22$. In panel (c), the experimental FS from panels (a) and (b) is overlaid. The points with error bars show the experimental FS. The solid line represents the LDA calculated FS with k_z integration included in the linewidth. The empty circles show $\mathbf{k}$-space locations where ARPES experiments have been performed. The data show remarkable symmetry with respect to Γ-G_1-Z high symmetry direction.

internal check of the sample orientation and data reproducibility and generates increased confidence in the data. The intensity of the photoemission peak, however, does not reflect the symmetry. This is most likely caused by a matrix element effect arising from the different photoelectron emission angles relative to the sample surface and incident photon direction.

Figure 2 presents the experimentally determined FS from the superconducting [Fig. 2(a)] and overdoped metallic [Fig. 2(b)] samples, together with the corresponding LDA calculated FS [20]. The solid line represents the calculated FS with k_z smearing included in the linewidth [21]. The experimental FS is marked with error bars with the orientation of each error bar along the direction of the slice in the Brillouin zone where the peak is observed to cross E_F. The empty circles indicate **k**-space locations where we have performed ARPES measurements, and their diameter represents the angular resolution of our spectrometer ($\pm 1°$). The experimentally determined FS for both doping levels agrees very well with results from the LDA calculations. Additional symmetry information obtained by changing the photon polarization, not shown here, also agrees with the calculated result that the band crossing E_F has antibonding $d_{x^2-y^2}$ symmetry [22].

The measured FS in NCCO provides the first opportunity to directly investigate the electronic structure of the CuO_2 plane since this is the first time the FS of a one-layer cuprate has been detected. Many theoretical models of the cuprates are based on the hypothesis that the essential physics are included in the nearest-neighbor interactions in the CuO_2 plane. A tight-binding calculation with only nearest-neighbors generates a square FS with perfect nesting along the [110] direction (Γ-X). By including the next-nearest-neighbor interactions, the FS is rotated by 45° and the corners of the square are rounded with strong nesting along the [100] direction (Γ-G_1) [23]. Our measured FS agrees with the latter scenario, suggesting that the next-nearest-neighbor interactions are very important to the electronic structure near E_F and model Hamiltonians including only nearest-neighbor interactions are not sufficient.

Figure 2(c) overlays the measured FS of the superconductor ($x=0.15$) and the metal ($x=0.22$). The data indicate that the FS of the metal is smaller, and tighter about the X point, than for the superconductor. Although the difference is only marginally beyond the experimental error bars, the internal check with respect to the Γ-G_1-Z line enhances the reliability of the conclusion. The trend towards a smaller FS with increased doping is qualitatively consistent with a band-filling scenario. In YBCO, the FS from CuO_2 planes was found to be insensitive to hole doping [14], so this is the first time a FS change with doping has been observed in the cuprates.

Despite the LDA calculation's remarkable success in predicting the FS, we found that it has difficulty describing the electronic structure below E_F. Figure 3 compares

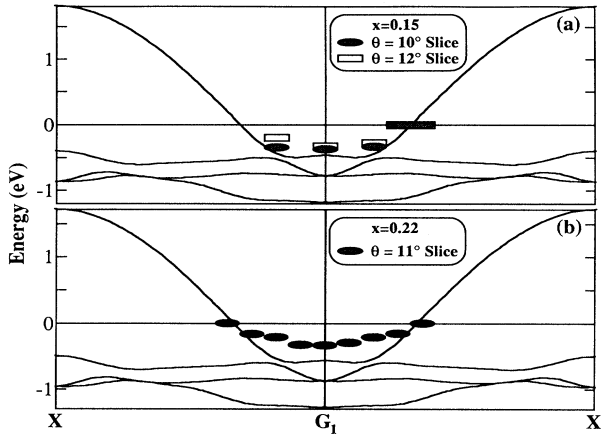

FIG. 3. Comparison of experimental and theoretical [20] E vs **k** relations for (a) $x=0.15$ and (b) $x=0.22$. Note that in panel (a) the data along $\theta=10°$ and $\theta=12°$ are slightly offset from the X-G_1-X high symmetry direction along $\theta=11°$.

the measured and LDA calculated band structure along the X-G_1X high symmetry direction. We again see an agreement between the measured and calculated FS crossing point. In disagreement with one-electron band theory, however, we find that for both samples the band is narrower than calculated along the X-G_1-X direction, a factor of 2 narrower for the metallic sample ($x=0.22$). In our full valence band data, which will be presented in a longer paper, our data show that aside from the band near E_F, there is virtually no spectral weight until a prominent feature near -2 eV binding energy, in contrast to the LDA prediction for this energy window. These discrepancies are most likely a result of the strong correlation effects arising from the large Coulomb U believed to be responsible for the insulating nature of undoped NCCO [24] and for the high energy satellite structure seen in both the insulating and superconducting phases of NCCO [25].

There are several important differences between the observed electronic structure of the n-type and p-type cuprates. First, we found that the ARPES peak is much broader near E_F than observed in YBCO and Bi2:2:1:2 (note that the experimental energy resolution is not the limiting factor here since the observed peak FWHM's are at least twice as broad as the instrumental resolution). The width of the peak was not found to be photon energy dependent. Second, a flat band and a corresponding high density of states near E_F, thought to originate from a van Hove singularity, is seen around G_1 in YBCO and Bi2:2:1:2 [13,18]. In NCCO, the flat part of the band is seen well below E_F (~ 300 meV), as expected because of the higher chemical potential. Finally, the FS of NCCO is very simple, in contrast to the much more complicated Fermi surfaces of YBCO and Bi2:2:1:2. This naturally leads us to question whether this simple FS and the absence of a high density of states at G_1 near E_F is linked to

the striking difference in physical properties between NCCO and the other cuprates. YBCO and Bi2:2:1:2, in addition to their extremely high T_c, exhibit some anomalous properties that raise questions about the applicability of conventional theories. Some examples include the linear temperature dependence of resistivity which casts doubt upon the validity of the Fermi-liquid picture [6], the anisotropy in the NMR relaxation rate which suggests d-wave superconductivity [7], the superconducting gap anisotropy seen in ARPES data from Bi2:2:1:2 which is more compatible with d-wave symmetry [8], and the temperature dependence of the penetration depth which cannot be fitted by a single s-wave gap [9]. This peculiar behavior of YBCO and Bi2:2:1:2 is in stark contrast to the more conventional behavior of NCCO: The resistivity has a T^2 temperature dependence [1–3], the tunneling data contain meaningful $\alpha^2F(\omega)$ information [4], and the penetration-depth temperature dependence can be fitted using a simple s-wave BCS picture [5].

It should be noted that the observed simple FS itself should not be interpreted as another piece of evidence for conventional behavior. In fact, it raises fundamental questions concerning the transport mechanisms in NCCO. The measured FS consists of a hole pocket centered at X, which according to semiclassical theory contains hole charge carriers. In disagreement with this prediction, the superconducting samples ($x=0.15$) have a negative Hall coefficient, revealing electron charge carriers [19,26]. The Hall sign becomes positive for overdoped metallic samples ($x \geq 0.20$); however, we do not see a large change in the shape of the FS to reflect the transition from hole to electron carriers. In addition, we find that for increased Ce doping, the Fermi surface shrinks. Therefore, we should expect the free carrier concentration to diminish. This is in contrast to both the resistivity and Hall coefficient measurements which decrease with increased Ce doping, consistent with a direct enhancement of the carrier density [19,26].

To determine whether the simpler electronic structure is connected to the more conventional physical properties of NCCO, more experiments and theoretical analysis are needed. First, a Cu NMR study of a n-type superconductor would be helpful to determine whether a simple s-wave BCS pair wave function is appropriate. Second, a detailed ARPES study of $La_{2-x}Sr_xCuO_4$ (LSCO), the p-type counterpart of NCCO also with one CuO_2 layer per unit cell, would test whether some aspect of the electronic structure is more complicated than for NCCO. For example, in LSCO a saddle point singularity, often called a van Hove singularity, is predicted at G_1 near E_F [20]. This would generate a large density of states near E_F at the same location in the Brillouin zone as already found in YBCO and Bi2:2:1:2. If the ARPES measurements on LSCO confirm the predicted high density of states near E_F at G_1, the connection between a possible van Hove singularity and the peculiar properties in the p-type cuprates is enhanced. On the theoretical side, we wonder whether the superconducting gap calculated using $V_{kk'}$, instead of V_0, would be strongly anisotropic for the more complicated FS of Bi2:2:1:2 and isotropic for the simpler FS of NCCO. This calculation would test whether the shape of the FS could be solely responsible for some of the distinctly different physical properties found in these two compounds. In any case, the simpler electronic structure observed in our experiment suggests that NCCO is an excellent candidate for detailed studies to understand the mechanism of superconductivity in cuprates since the data interpretation and theoretical calculations are much simpler.

The data presented here were obtained from the Stanford Synchrotron Radiation Laboratory (SSRL) which is operated by the DOE Office of Basic Energy Sciences, Division of Chemical Sciences. The Office's Division of Materials Science has provided support for this research. The Stanford work was also supported by NSF Grants No. DMR8913478 and No. DMR9121288, and the NSF grant through the Center of Materials Research. Beam line 5 of SSRL was built with DARPA, ONR, AFOSR, AOR, DOE, and NSF support. The University of Maryland work was supported by NSF Grant No. DMR911-5384. We are grateful to Jaejun Yu and A. J. Freeman for providing us with additional results from their LDA calculations.

[1] C. C. Tsuei *et al.*, Physica (Amsterdam) **161C**, 415 (1989).
[2] Y. Hidaka and M. Suzuki, Nature (London) **338**, 635 (1989).
[3] S. J. Hagen *et al.*, Phys. Rev. B **43**, 13606 (1991).
[4] Q. Huang *et al.*, Nature (London) **347**, 369 (1990).
[5] D. H. Wu *et al.*, Phys. Rev. Lett. **70**, 85 (1993).
[6] P. W. Anderson, Science **256**, 1526 (1992).
[7] P. Monthoux *et al.*, Phys. Rev. Lett. **67**, 3448 (1991).
[8] B. O. Wells *et al.*, Phys. Rev. B **46**, 11830 (1992).
[9] S. M. Anlage *et al.*, Phys. Rev. B **44**, 9764 (1991).
[10] C. G. Olson *et al.*, Science **245**, 731 (1989).
[11] B. O. Wells *et al.*, Phys. Rev. Lett. **65**, 3056 (1990).
[12] J. C. Campuzano *et al.*, Phys. Rev. Lett. **64**, 2308 (1990).
[13] J. G. Tobin *et al.*, Phys. Rev. B **45**, 5563 (1992).
[14] R. Liu *et al.*, Phys. Rev. B **45**, 5614 (1992).
[15] C. M. Fowler *et al.*, Phys. Rev. Lett. **68**, 534 (1992).
[16] H. Haghihi *et al.*, Phys. Rev. Lett. **67**, 382 (1991).
[17] Y. Sakisaka *et al.*, Phys. Rev. B **42**, 4189 (1990).
[18] D. S. Dessau (unpublished).
[19] J. L. Peng *et al.*, Physica (Amsterdam) **177C**, 79 (1991).
[20] S. Massidda *et al.*, Physica (Amsterdam) **157C**, 571 (1989).
[21] Note, we have projected the Fermi surfaces for $k_z=0$, $\pi/2c$, and π/c to represent the calculated Fermi surface in the 2D figure.
[22] D. M. King (unpublished).
[23] J. Yu *et al.*, J. Phys. Chem. Solids **52**, 1351 (1991).
[24] M. B. Maple, MRS Bull. **XV**, 60 (1990).
[25] J. W. Allen *et al.*, Phys. Rev. Lett. **64**, 595 (1990).
[26] S. J. Hagen *et al.*, Phys. Rev. B **43**, 13606 (1991).